CHARACTERIZATION OF THE N- AND C-TERMINAL SUMO INTERACTING MOTIFS OF THE SCAFFOLD PROTEIN DAXX

Eric Escobar-Cabrera, Mark Okon, Desmond K. W. Lau,
Christopher F. Dart, Alexandre M.J.J. Bonvin, and Lawrence P. McIntosh

SUPPLEMENTAL DATA

Supplemental Table S1. Sample conditions used for titrations. [a]

[KCl] (mM)	Labeled-species	Conc. (mM) [b]	Unlabeled species	Conc. (mM)	Final volume added (μL) / ratio ^{15}N species :unlabeled species
0	SUMO-1	0.13	SIM-N	3.0	32 / 1 : 1.5
100	SUMO-1	0.15	DAXX$^{1-144}$	2.1	292 / 1 : 8.3
0	SUMO-2	0.10	SIM-N	3.0	27 / 1 : 1.6
100	SIM-N	0.12	SUMO-1	2.5	130 / 1 : 5.5
100	SIM-N	0.12	SUMO-2	2.5	130 / 1 : 5.5
200	SIM-N	0.09	SUMO-1	2.3	112 / 1 : 5.8
200	SIM-N	0.14	SUMO-2	8.7	120 / 1 : 15.5
0	SIM-C	0.11	SUMO-1	1.7	142 / 1 : 4.4
0	SIM-C	0.11	SUMO-2	1.7	142 / 1 : 4.4
100	SIM-C	0.13	SUMO-1	2.2	220 / 1 : 7.8
100	SIM-C	0.13	SUMO-2	1.7	250 / 1 : 6.8
200	SIM-C	0.09	SUMO-1	2.3	240 / 1 : 12
200	SIM-C	0.13	SUMO-2	8.7	180 / 1 : 24

[a] Samples at 25 °C in an NMR buffer composed of ~5% D_2O, 10 mM K_2HPO_4, 0.1 mM EDTA, 10 mM DTT, pH 6.5 and the indicated KCl concentration.

[b] Initial volume 500 μL.

Supplemental Table S2. Intermolecular NOEs between unlabeled SIM-N and $^{13}C/^{15}N$ labeled SUMO-1.

$^{13}C/^{15}N$ SUMO-1		unlabeled SIM-N	
I34	$H^{\gamma 2}$	I8	H^{α}, $H^{\gamma 2}$, $H^{\delta 1}$; V9 H^{α}
H35	H^{N}	I8	H^{α}, $H^{\gamma 2}$
H35	$H^{\beta 1}$, $H^{\beta 2}$	I8	H^{α}, $H^{\gamma 2}$
F36	$H^{\beta 1}$, $H^{\beta 2}$	L10	$H^{\delta 2}$
F36 (or 35) aromatic		L10	$H^{\beta 1}$, $H^{\beta 2}$; V9 $H^{\gamma 1,2}$; I8 $H^{\delta 1}$
K37	H^{N}	L10	H^{α}, $H^{\delta 2}$
K37	$H^{\beta 1}$, $H^{\beta 2}$	V9	$H^{\gamma(1or2)}$; L10 $H^{\delta 2}$
K37	$H^{\gamma 1}$, $H^{\gamma 2}$	L10	$H^{\delta 2}$
V38	$H^{\delta(1or2)}$	L10	$H^{\delta 1}$, $H^{\delta 2}$
V39	H^{β}	D11	$H^{\beta 2}$
V39	H^{β}	L10	$H^{\delta 1}$, $H^{\delta 2}$
T42	$H^{\gamma 2}$	L10	$H^{\delta 2}$; D11 H^{β}
H43	H^{N}	D11	H^{α}, $H^{\beta 2}$
L47	H^{N}	L10	$H^{\delta 1}$, $H^{\delta 2}$
L47	H^{α}	L10	$H^{\delta 1}$, $H^{\delta 2}$
L47	$H^{\delta 1}$	L10	$H^{\delta 2}$
S50	H^{N}	L10	$H^{\delta 1}$, $H^{\delta 2}$
R54	$H^{\beta 1}$	I8	$H^{\delta 1}$
R54	$H^{\beta 2}$	I7 or I8	$H^{\gamma 2}$
R54	$H^{\delta 1}$	I8	$H^{\delta 1}$

Supplemental Table S3. Statistics for HADDOCK structure calculations.

	SIM-N/DHB[a]	SIM-N/SUMO-1	SIM-C/SUMO-1 3 body[b]	SIM-C/SUMO-1 2 body[c]
Number of clusters	15	2	4	1
Cluster rank	1	1	1	1
Cluster population	5	190	166	198
RMSD from overall lowest-energy structure (Å)	2.2 ± 1.5	2.8 ± 1.7	2.1 ± 1.3	0.9 ± 0.5
HADDOCK score (a.u.)	-127.8 ± 17.4	-104.7 ± 3.9	-139.4 ± 4.1	99.5 ± 9.9
van der Waals energy (kcal mol^{-1})	-58.4 ± 9.3	-51.1 ± 10.5	-52.4 ± 13.3	-32.2 ± 3.3
Electrostatic energy (kcal mol^{-1})	-563.0 ± 90.3	-371.7 ± 25.8	-652.4 ± 106.7	-257.5 ± 19.2
Desolvation energy (kcal mol^{-1})	30.0 ± 7.2	16.1 ± 2.4	35.5 ± 9.0	18.3 ± 7.4
Restraints violation energy (kcal mol^{-1})	132.3 ± 40.8	46.2 ± 14.2	8.0 ± 5.8	165.0 ± 11.9
Buried surface area ($Å^2$)	1868 ± 169	1276 ± 69	2584 ± 126	1069 ± 42

[a] Only ambiguous interaction restraints were used.

[b] Ensemble averaged three body docking with two copies of the SIM-C peptide. The PRE restraints were calculated as ensemble average over the two peptides. In each resulting complex, one peptide bound in the parallel mode and the other antiparallel.

[c] Regular two body docking with only one copy of the SUMO-1 peptide. Only the parallel binding orientation was observed. Note the high restraint energy compared to the ensemble averaged docking run.

Supplemental Table S4. Summary of reported dissociation constants of SIM/SUMO complexes. [a]

SUMO paralog	SIM [b]	K_D (μM)	Buffer	Reference
SUMO-1	PIASX-Pa	7	20 mM Tris, pH 7.6, 30 °C	(1)
SUMO-1	PIASX-N	9	20 mM Tris, pH 7.6, 30 °C	(1)
SUMO-3	PIASX-N	5	20 mM Tris, pH 7.6, 30 °C	(1)
SUMO-1	PIASX-Pb	6	20 mM phosphate, pH 7.4, 30 °C	(2)
SUMO-1	MCAF1	14	20 mM phosphate, pH 6.8, 25 °C	(3)
SUMO-1	MCAF1	12 [c]	20 mM phosphate, pH 6.8, 25 °C 150 mM NaCl	(3)
SUMO-1	MCAF1	8 [c]	20 mM phosphate, pH 6.8, 25 °C 300 mM NaCl	(3)
SUMO-3	MCAF1	1.3	20 mM phosphate, pH 6.8, 25 °C	(3)
SUMO-3	MCAF1	1.1 [c]	20 mM phosphate, pH 6.8, 25 °C 150 mM NaCl	(3)
SUMO-3	MCAF1	N.D. [d]	20 mM phosphate, pH 6.8, 25 °C 300 mM NaCl	(3)

[a] All reported dissociation constants were measured with ITC.

[b] **PIASX-Pa:** KVDVIDLTIESSSDEEEEDPPAKR;
PIASX-N: VDVIDLTIE;
PIASX-Pb: KVDVIDLTIE
MCAF-1: GVIDLTMDDEE

[c] Noisy binding curve.

[d] Not determined due to no significant heat release.

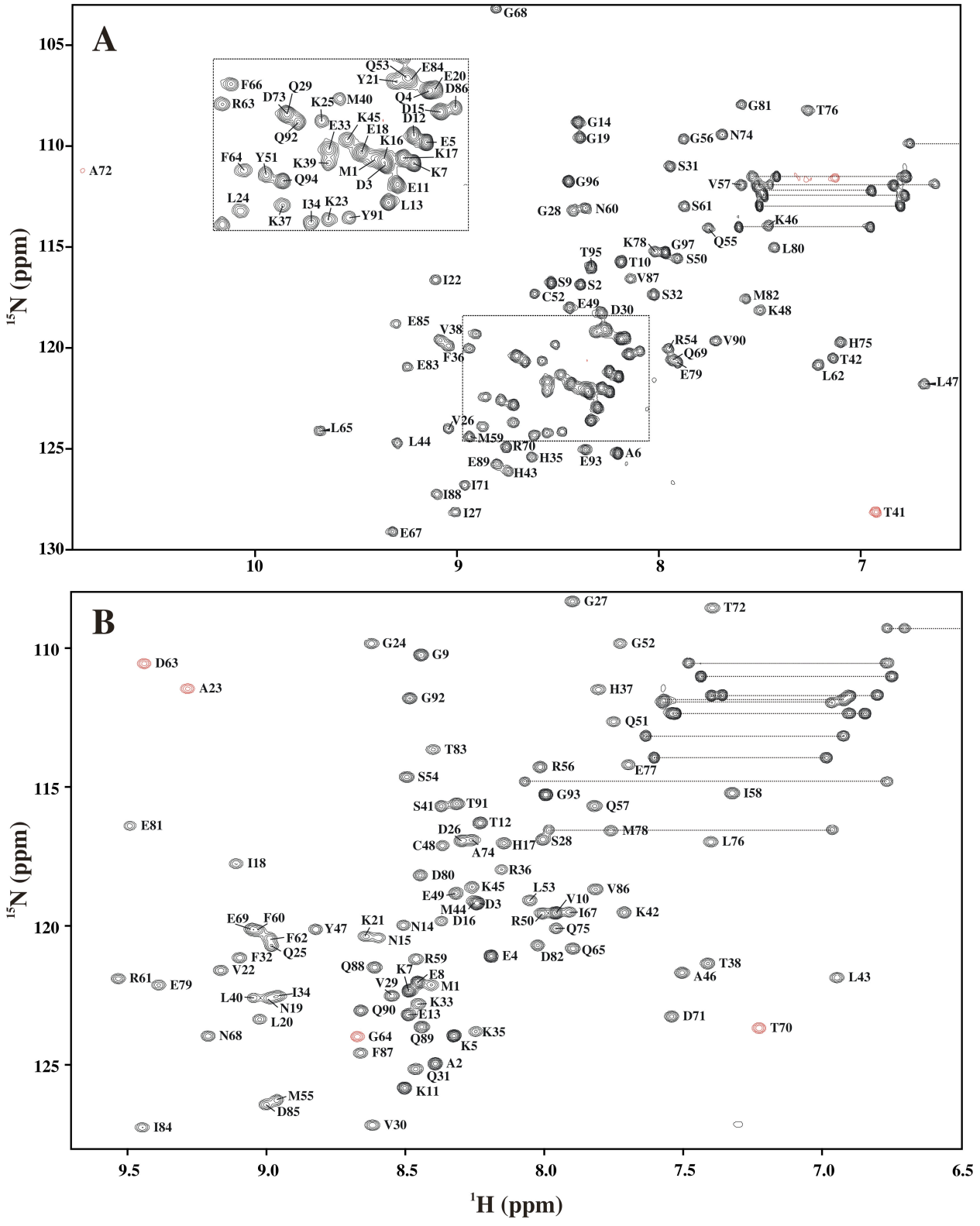
A
B
^{15}N (ppm)
^{1}H (ppm)

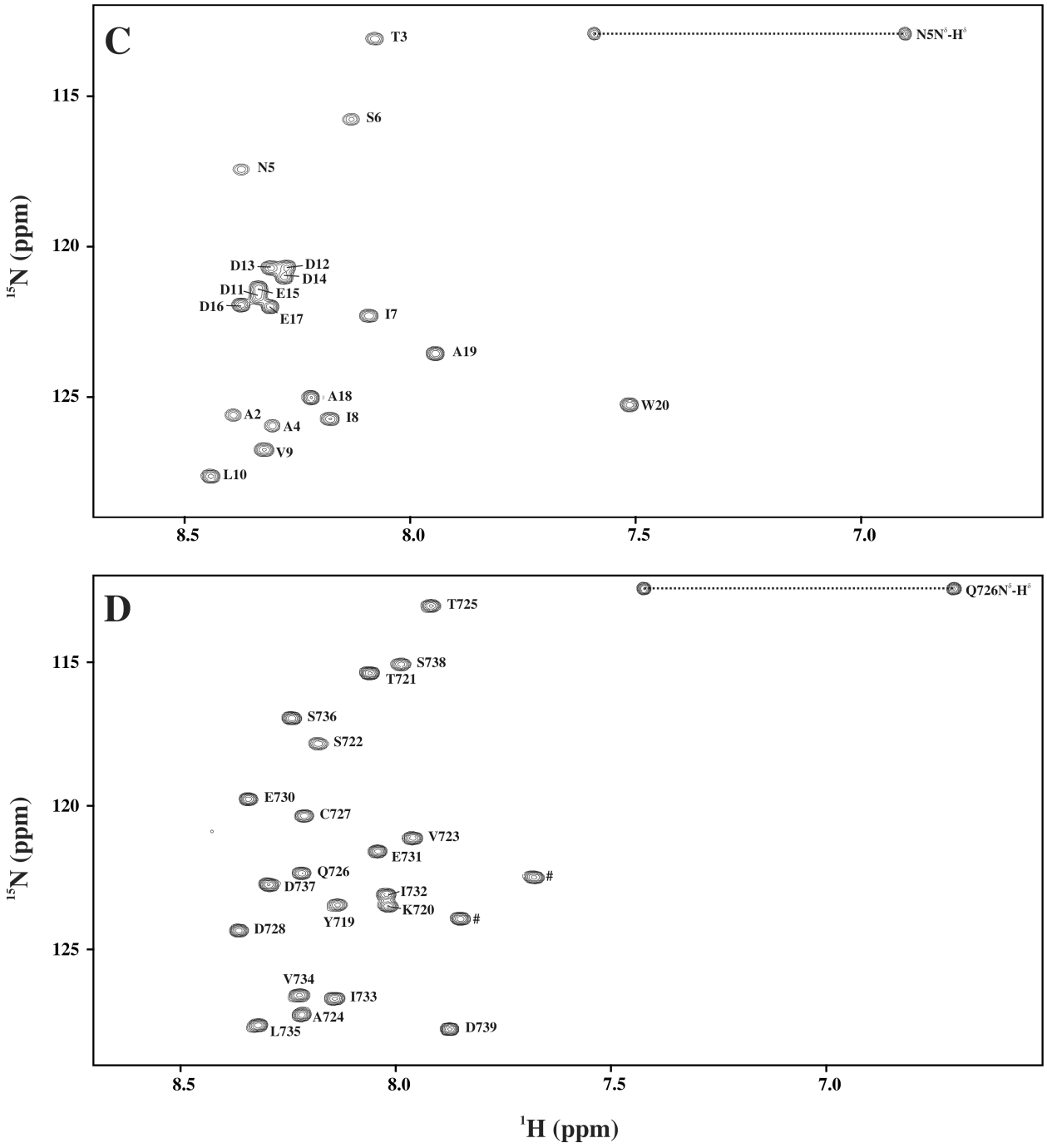

Supplemental Figure S1. Annotated ^{1}H-^{15}N HSQC spectra of (**A**) SUMO-1 (155 μM, 17 °C), (**B**) SUMO-2 (1.1 mM, 25 °C), (**C**) SIM-N (120 μM, 25 °C), and (**D**) SIM-C (125 μM, 25 °C). All samples were in common buffer (10 mM phosphate, 100 mM KCl, 0.1 mM EDTA, pH 6.5). The signals from Asn and Gln side-chain $^{15}NH_2$ groups are connected by horizontal lines. Aliased peaks are shown in red. Peaks in (D) marked as # correspond to either W718 or I719.

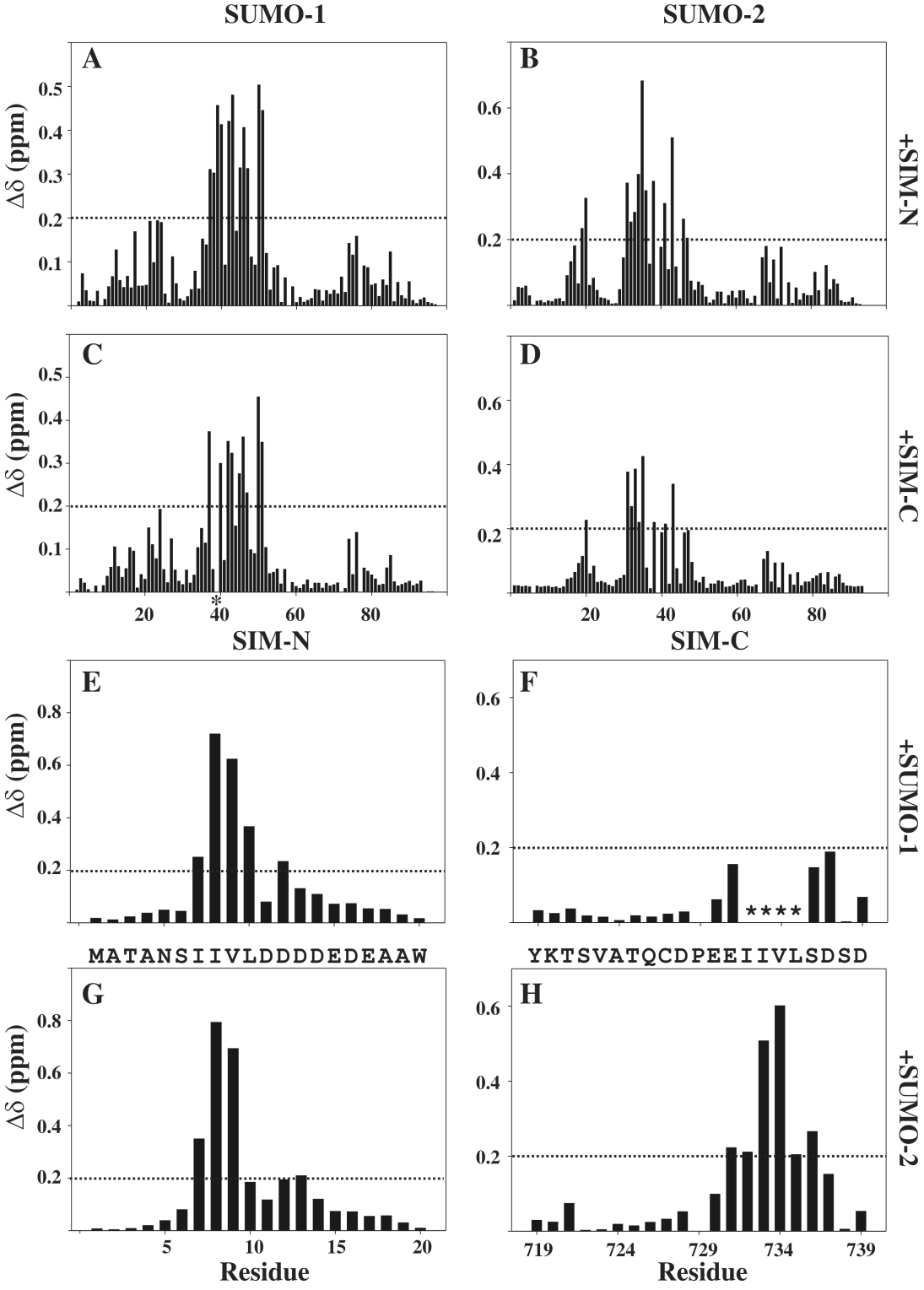

Supplemental Figure S2. Mapping the binding interfaces of SUMO-1 and SUMO-2 with SIM-N and SIM-C. Amide chemical shift perturbations of (**A,C**) SUMO-1 and (**B,D**) SUMO-2 upon binding (**A,B**) SIM-N and (**C,D**) SIM-C. Also shown are (**E,G**) SIM-N and (**F,H**) SIM-C amide chemical shift changes upon binding (**E,F**) SUMO-1 and (**G,H**) SUMO-2. The signals of

residues marked as * were broadened beyond detection in the complex. All samples were in 10 mM potassium phosphate, 0.1 mM EDTA, 5 mM DTT, pH 6.5, with 0 (A, B) or 100 mM KCl (C-H) at 25 °C. The dashed lines show the cut-off values for residues highlighted in Figure 3. Supplemental Table S1 summarizes the final SIM/SUMO ratios in the spectra used to obtain these chemical shift perturbation values.

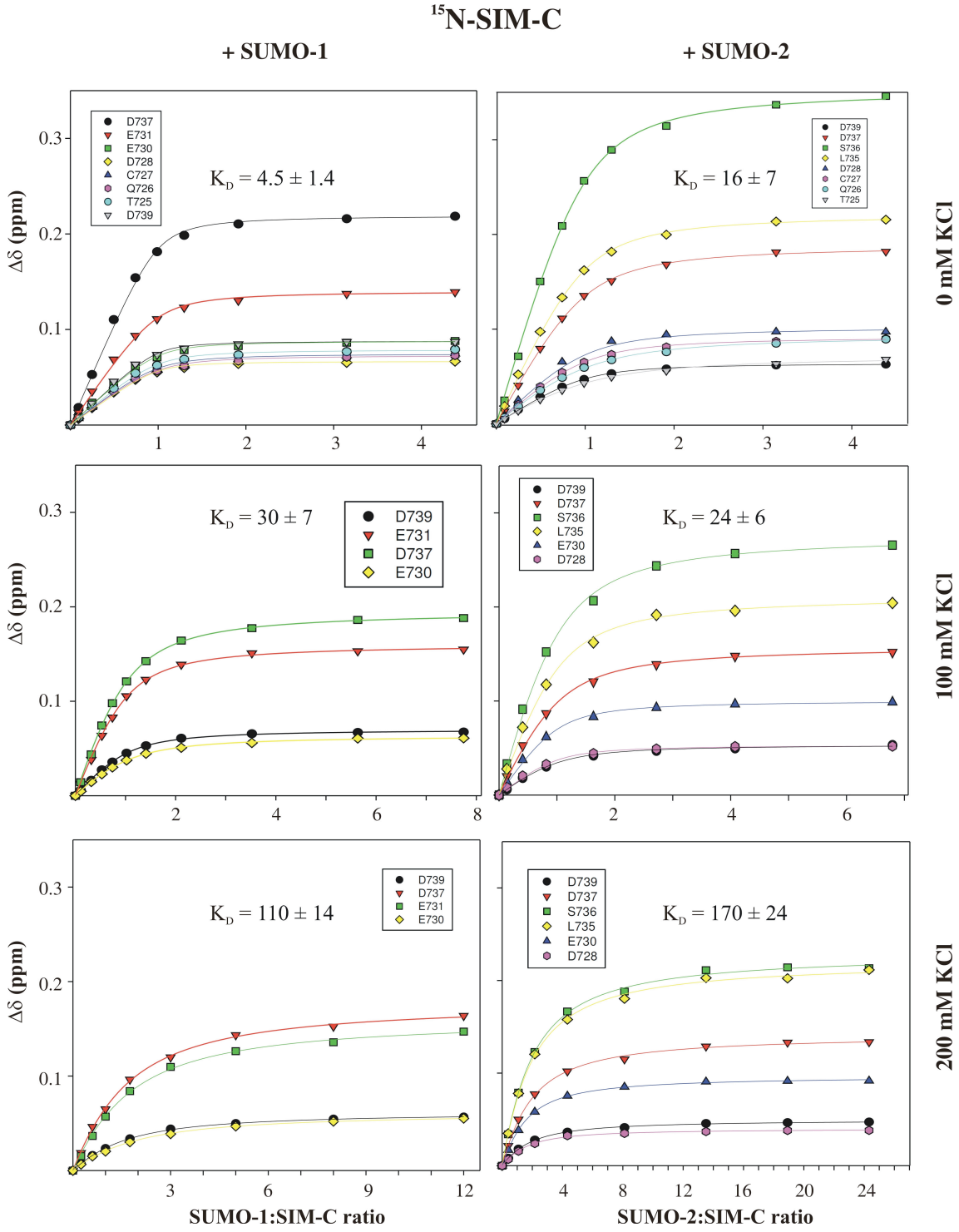
15N-SIM-C
+ SUMO-1
+ SUMO-2
0 mM KCl
100 mM KCl
200 mM KCl
Δδ (ppm)
K_D = 4.5 ± 1.4
K_D = 16 ± 7
K_D = 30 ± 7
K_D = 24 ± 6
K_D = 110 ± 14
K_D = 170 ± 24
D737
E731
E730
D728
C727
Q726
T725
D739
S736
L735
SUMO-1:SIM-C ratio
SUMO-2:SIM-C ratio

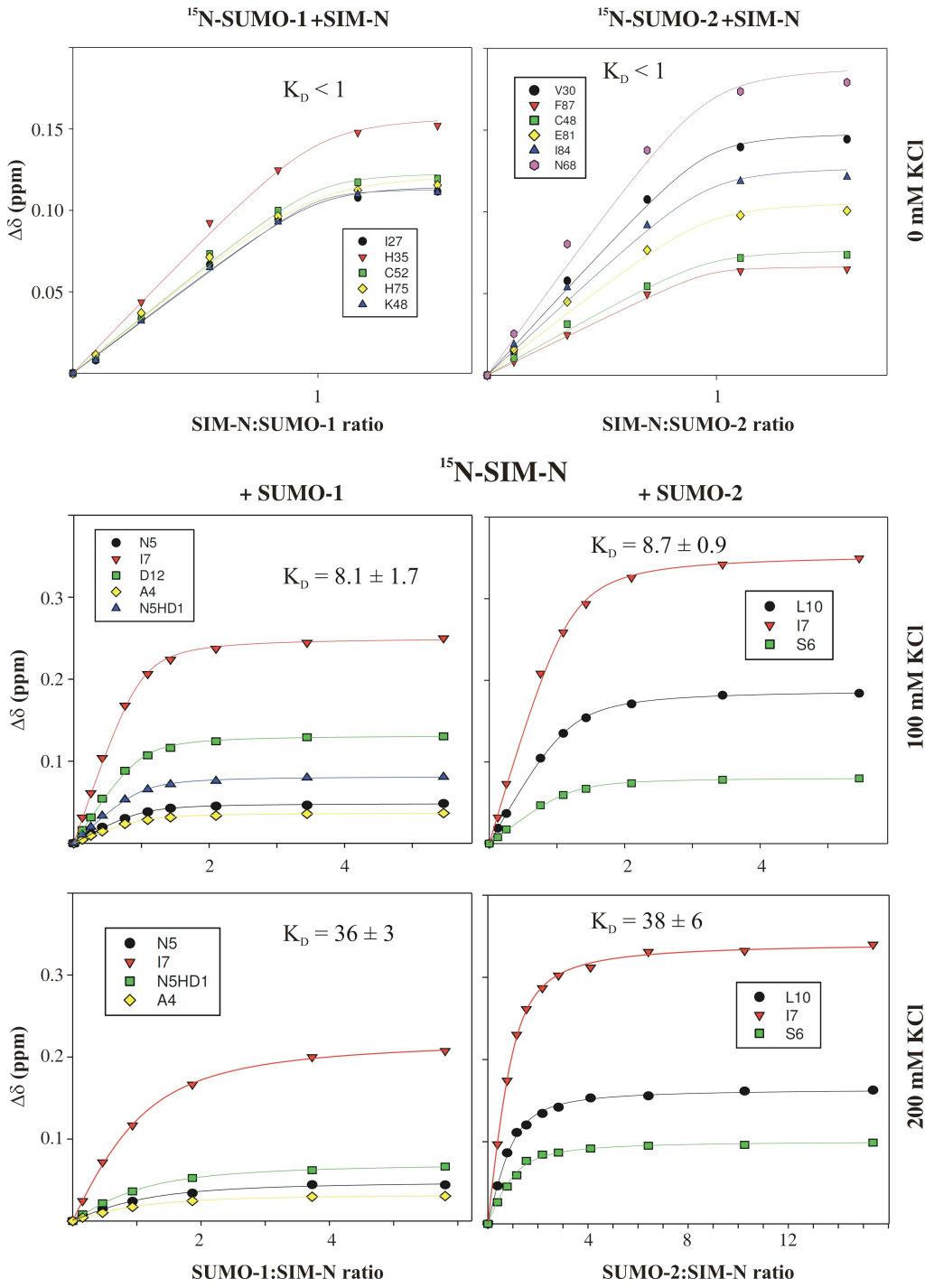

Supplemental Figure S3. Titration curves used to determine K_D values. The dissociation constants reported in Table 1 were derived using data from the titrations shown in Figures 1 and 2. The regressions were calculated using the equation for formation of a 1:1 complex in the fast exchange limit (4), with protein and peptide concentrations summarized in Supplemental Table S1. Average values ± standard deviations are derived from the individual fits for the indicated residues. The plots for ^{15}N-labeled SUMO-1 and SUMO-2 with unlabelled SIM-N showed stoichiometric binding, so only an upper estimate for the K_D was obtained.

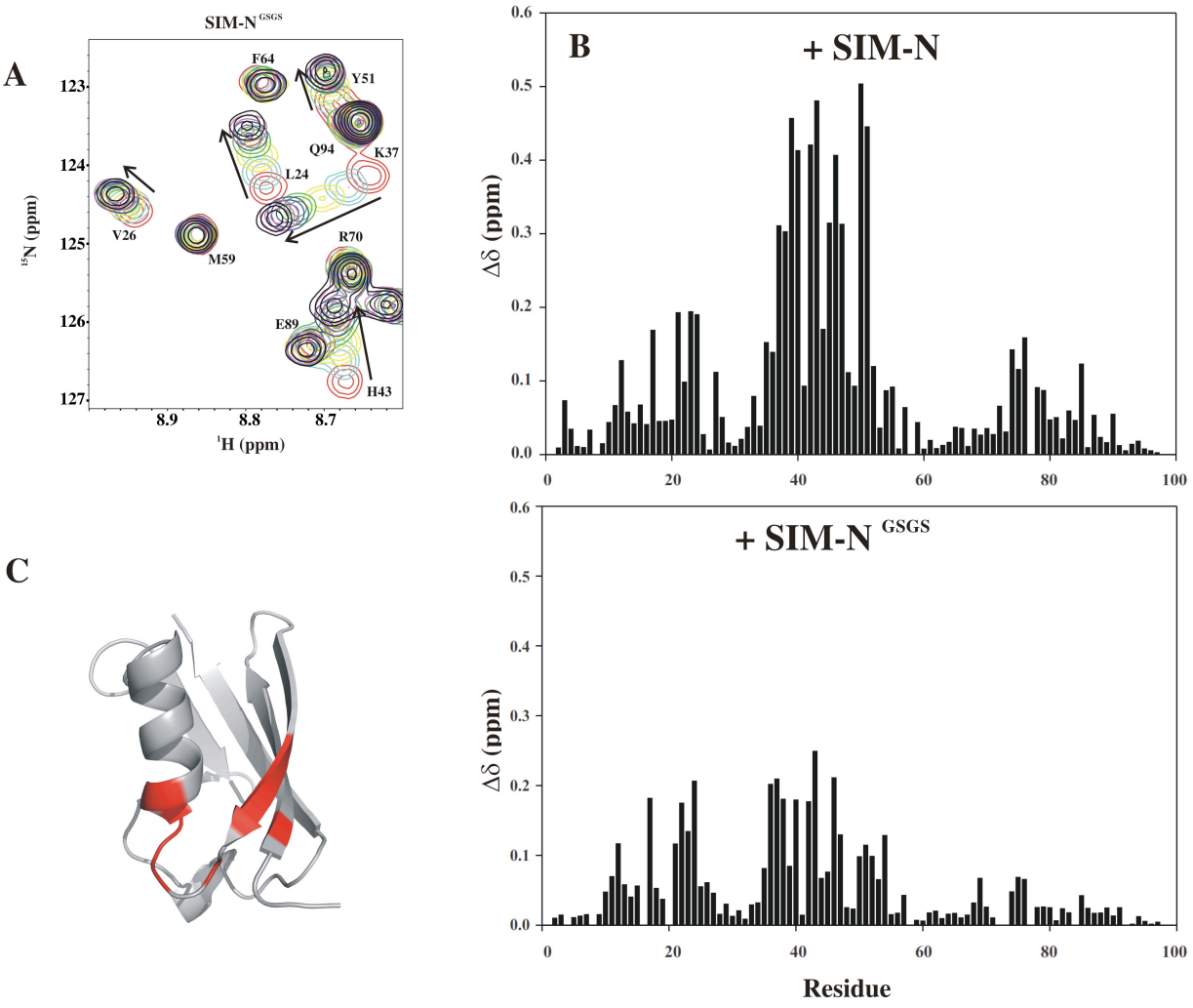

Supplemental Figure S4. NMR-monitored titration of SUMO-1 with SIM-N^{GSGS} demonstrates that a SIM mutant lacking the hydrophobic core Ile-Ile-Val-Leu still weakly binds SUMO-1 between helix α1 and stand β2. **(A)** Section of the overlapped ^{15}N-HSQC spectra of ^{15}N-SUMO-1 with increasing amounts of unlabeled SIM-N^{GSGS}. Arrows show peaks shifting as the concentration of SIM-N^{GSGS} increases from 0 (red) up to a stoichiometric ratio of 16:1 (black). (**B**) Comparison of the SUMO-1 amide chemical shift perturbations upon addition of a 1.5 molar excess of SIM-N (top) and a 16 fold excess of SIM-N^{GSGS} (bottom). (**C**) Mapping of SUMO-1 residues showing the greatest chemical shift perturbation (< 0.12 ppm) upon binding SIM-N^{GSGS} confirms the binding site. Fitting the titration data yielded a K_D = 440 ± 30 μM.

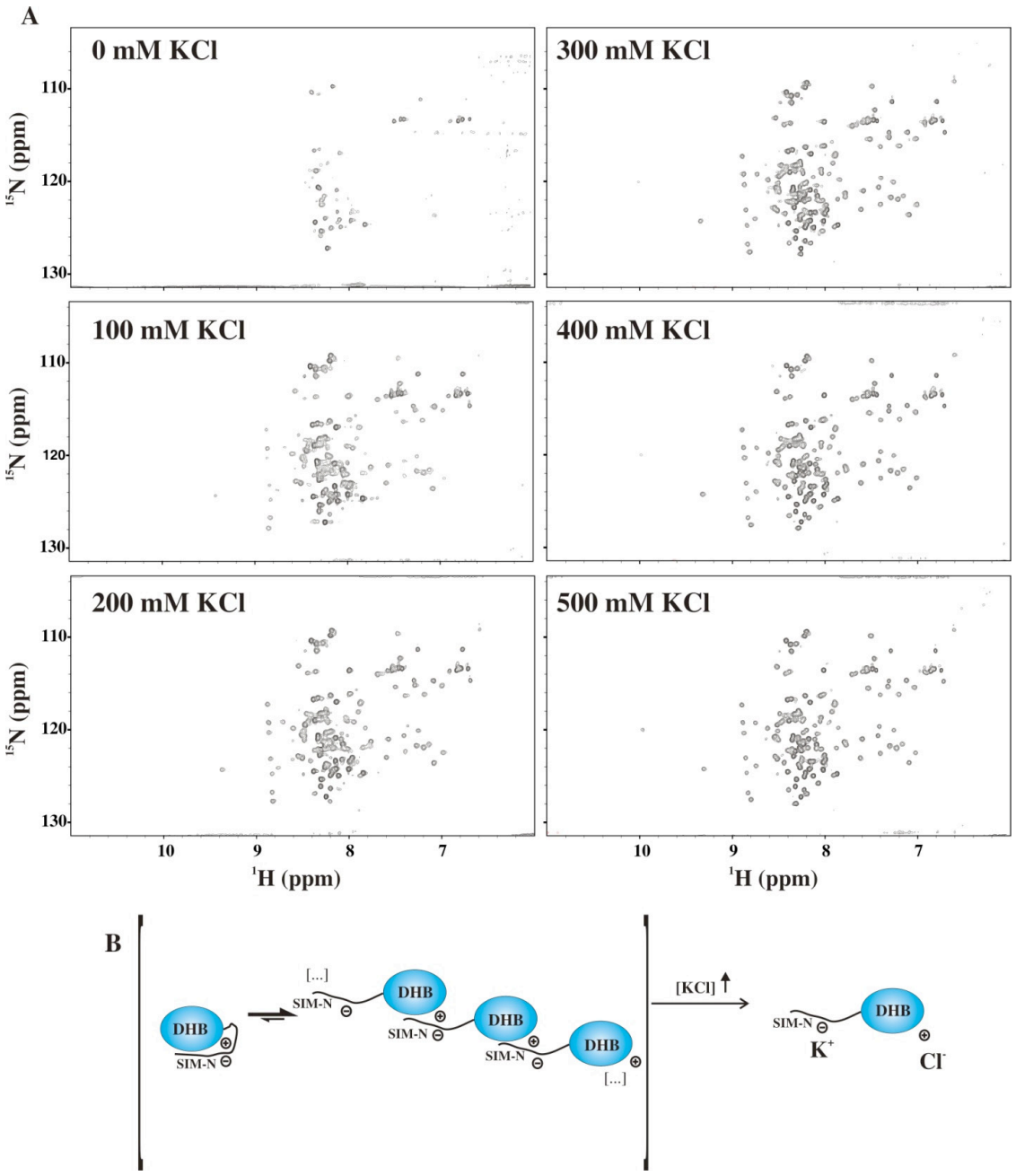

Supplemental Figure S5. DAXX$^{1\text{-}144}$ self-association is ionic strength dependent. (**A**) The ^{15}N-HSQC spectra of DAXX$^{1\text{-}144}$ showed broad and missing peaks at low ionic strength. As the KCl concentration was increased, $^{1}H^{N}$-^{15}N peaks reappeared and became sharper. (**B**) At low ionic strength and a relatively high concentration of DAXX$^{1\text{-}144}$ (100 μM), intermolecular binding of the SIM-N and DHB domain to form multimers is presumably favored, whereas at high ionic strength, the monomer is favored.

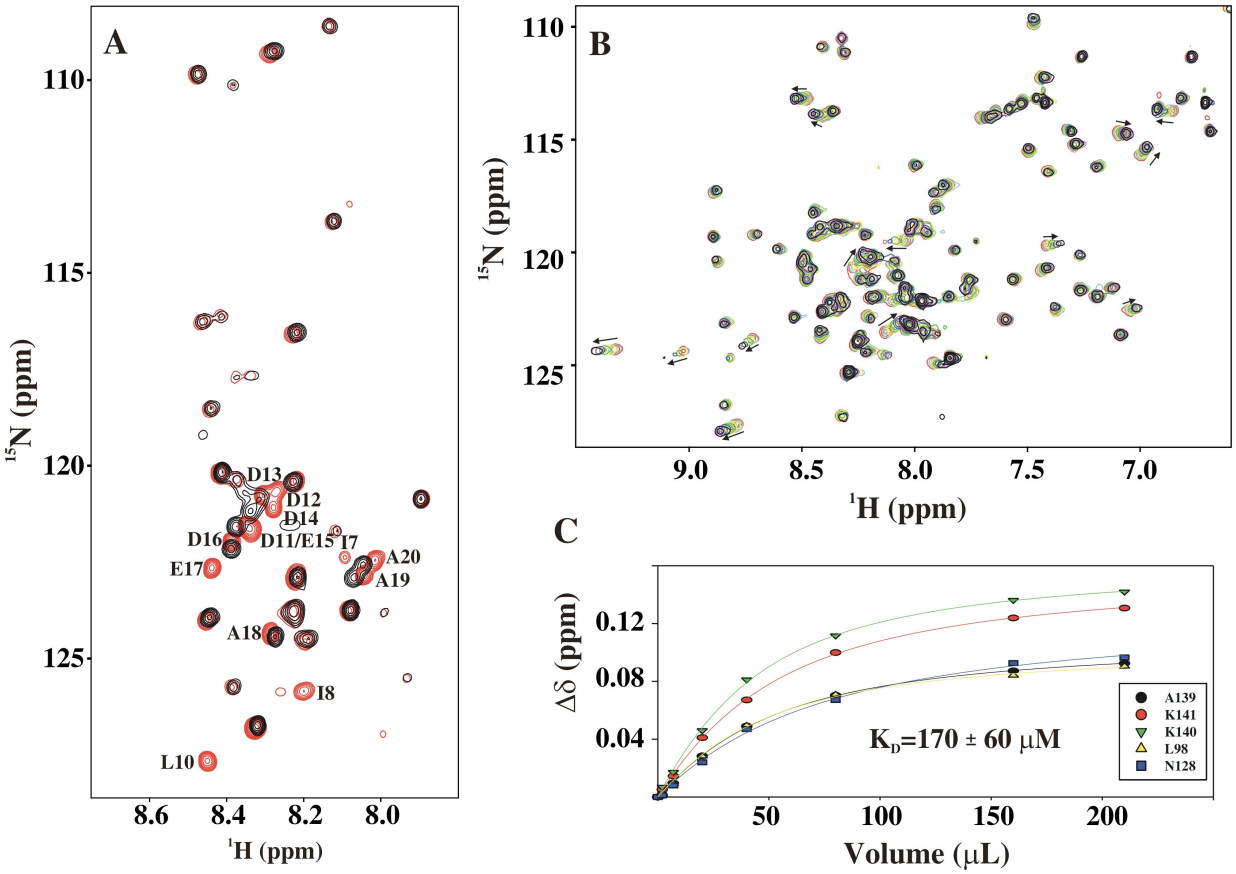

Supplemental Figure S6. SIM-N in DAXX$^{1-56}$ binds the DHB domain of DAXX$^{55-144}$. (**A**) Superimposed ^{15}N-HSQC spectra of DAXX$^{1-56}$ in the absence (initially 150 μM in 500 μL, red) and presence of unlabeled DAXX$^{55-144}$ (250 μL of 1.4 mM stock added, black). The assigned residues showing the most significant changes (broadening) correspond to those of SIM-N within DAXX$^{1-56}$. (**B**) Reciprocal titration of ^{15}N-DAXX$^{55-144}$ (140 μM in 500 μL) with progressive aliquots of unlabeled DAXX$^{1-56}$ confirmed binding (210 μL of 2.2 mM stock added). Arrows indicate amide peaks undergoing chemical shift changes upon addition of DAXX$^{1-56}$. (**C**) The dissociation constant (170 ± 60 μM) was calculated from fitting individually the chemical shift changes for the five indicated amides of ^{15}N-DAXX$^{55-144}$.

SUPPLEMENTAL REFERENCES

1. Song, J., Durrin, L. K., Wilkinson, T. A., Krontiris, T. G., and Chen, Y. A. (2004) *Proc. Natl. Acad. Sci. U. S. A.* **101**, 14373-14378

2. Song, J., Zhang, Z., Hu, W., and Chen, Y. (2005) *J. Biol. Chem.* **280**, 40122-40129

3. Sekiyama, N., Ikegami, T., Yamane, T., Ikeguchi, M., Uchimura, Y., Baba, D., Ariyoshi, M., Tochio, H., Saitoh, H., and Shirakawa, M. (2008) *J. Biol. Chem.* **283**, 35966-35975

4. Johnson, P. E., Tomme, P., Joshi, M. D., and McIntosh, L. P. (1996) *Biochemistry* **35**, 13895-13906